Dynamics of delaminated elements of smart structures

A. TYLIKOWSKI

Warsaw University of Technology
Narbutta 84, 02–524 Warszawa, Poland
e-mail: aty@simr.pw.edu.pl

The purpose of this work is to show an influence of interlayer separations on dynamic behaviour of simple laminated elements of smart structures. A general bending – extensional model of the response of a simple laminated structures to excitation by an nonsymmetric actuator made using piezoelectric elements is presented. The edge delamination is modeled by hanging the effective length of debonded actuator. Dynamic equations, joints conditions between sections with and without active layers as well as the boundary conditions at the two ends of the beam form a boundary value problem. The dynamic extensional strain on the beam surface is calculated by including the free stress conditions at the piezoelectric actuator boundaries, by considering the dynamic coupling between the actuator and the beam, and by taking into account a finite bonding layer with the finite stiffness. The analysis indicates that the edge delamination has a harmful effect on the performance of piezo-actuators, but the significant decrease of natural frequencies with an increase of delamination length is not observed. The influence of the delamination length on the system transfer functions (the beam surface strain, the beam transverse displacement and the shear stresses in bonding layers) is shown. The dynamics and stability of rotating hybrid shafts with delaminations is also presented. The composite thin-walled rotating shaft, treated as a symmetrically laminated shell, contains both the conventional (e.g. graphite or glass) angle-ply layers and the activated shape memory alloy fibers parallel to the shaft axis. The results indicate that the delamination significantly decrease the critical angular velocity.

Key words: *active damping, piezoelectric actuators, delaminations, rotating shaft, thermal activation*

1. Introduction

Piezoelectric materials show great advantages as actuators in intelligent structures i.e. structures with highly distributed actuators, sensors, and processor networks. Piezoelectric sensors and actuators have been applied successfully in the closed loop control [1, 7]. The beam vibration due to the excitation of a piezoelectric actuator has been modelled [3, 5]. In particular, a comprehensive static model for a piezoelectric actuator glued to a beam has been presented. The relationship between static structural strains, both in the structure and in the actuator, and the applied voltage across the piezoelectric was presented. This static approach was then used to predict the dynamic behavior. As the shear modulus of bonding layers increases or the thickness of bonding layers decreases the shear lag becomes less significant and the shear stresses are transferred from actuators to the beam over small regions close to the piezoelectric ends.

For the perfectly bonding layers the tangential stress distribution is described by the two Dirac-delta functions located at the piezoelement ends. High shear stresses can cause a crack initiation and propagations in bonding layer, delamination or even total debonding of piezoelectric element. A dynamic model for a simply supported beam with a piezoelectric actuator glued to each of its upper and lower surfaces was developed [5]. In the model the actuators were assumed to be perfectly bonded. It means that the bonding layer is sufficiently thin that the shear of layer can be neglected. The effect of through-width delamination on the vibration characteristics of laminated beam without piezo-actuators was studied [6]. The influence of composite plate delamination on buckling of the debonded layers was discussed [4]. Analysis performed in [2] shows that complete and accurate solving of bonded plates can be only obtained in 3-D elasticity formulation and numerical solutions. The effects of delamination on the performance of piezo-actuators which are surface mounted on a cantilever beam assuming a pure bending model and the mass per unit area of the piezoelement and the beam equal to one was investigated [8]. It was shown that the edge delamination significantly decreases the coupling performance of piezo-actuators.

In the present paper, a bending – extensional dynamic model of the beam-bonding layer-actuators system is proposed. The pure extensional strain in the piezoelectric elements and the massless bonding layers are assumed. The dynamic extensional strain on the beam surface is calculated by including the free stress conditions at the piezoelectric actuator boundaries, by considering the dynamic coupling between the actuator and the beam, and by taking into account a finite bonding layer with the finite stiffness. The approach has been used in [9] to derive a control strategy especially useful in collocated sensor-actuator systems. The used dynamic equations can be reduced to the particular cases from past studies, which were based on the assumption of static coupling between the actuator and the beam or assuming the perfect bonding in dynamical analysis.

2. Effects of piezo-actuator delamination

2.1. Analysis

Consider the elastic beam with the identical piezoelectric layers mounted on each of two opposite sides. Figure 1 shows an edge delamination of the lower piezo-actuator. For simplicity, it is also assumed that the gap width extends uniformly across the beam [8].
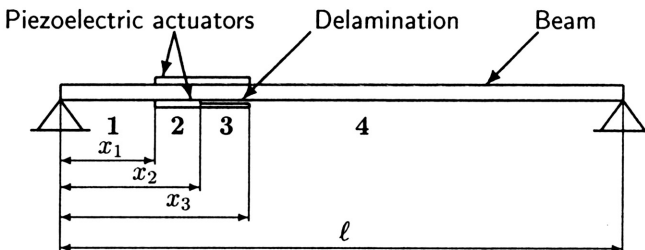

FIGURE 1. Beam with partially debonded piezoelectric layers.

The analysis will use the Bernoulli-Euler theory to describe a beam motion. The beam is assumed to be simply supported. Due to the geometry the beam is divided into four parts as shown in Fig. 1, and the dynamic behavior of each part is described by different equations [11].

The motion is describeded by the beam transverse displacement w due to bending and the pure longitudinal displacements u_{pe}^+ and u_{pe}^- of upper and lower piezoelectric actuators, respectively. The poling directions in both actuators are the same. The actuators are driven by a pair of electrical fields $\mathcal{V}$ with the same amplitude and in opposite phase. The inertia forces of finite-thickness bonding layers are neglected and the pure one-dimensional shear in the bonding layer is assumed. Consider an infinite element of beam and upper and lower actuators in the second section $x_1 < x < x_2$ shown in Fig. 2. The thickness of beam, bonding layer and piezoelectric actuator is denoted by t_b, t_s, t_{pe}, respectively.
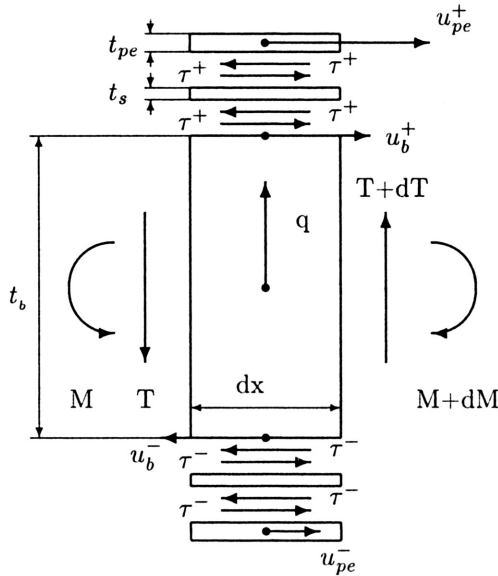

FIGURE 2. Geometry of the beam in the second section.

The beam dynamics equations are as follows

$$T_{,x} - \rho_b^* t_b b w_{,tt} = 0, \tag{1}$$

$$M_{,x} - T + b t_b (\tau^+ + \tau^-) = 0, \tag{2}$$

where $\rho_b^* = \rho_b(1 + 2\frac{\rho_{pe} t_{pe}}{\rho_b t_b})$ is the equivalent beam density, and the subscript comma denotes partial differentiation with respect to the variable after comma. Under the assumption of pure extensional strains in the piezoelectric elements their dynamic equations expressed by longitudinal strains $\varepsilon^+ = u_{pe,x}^+$, $\varepsilon^- = u_{pe,x}^-$ are

$$\rho_{pe} t_{pe} \varepsilon_{,tt}^+ - E_{pe} t_{pe} \varepsilon_{,xx}^+ + \tau_{,x}^+ = 0, \tag{3}$$

$$\rho_{pe} t_{pe} \varepsilon_{,tt}^- - E_{pe} t_{pe} \varepsilon_{,xx}^- + \tau_{,x}^- = 0. \tag{4}$$

For the massless bonding layers isotropic stress-strain relations are

$$\tau^+ = \frac{G}{t_s}(u_{pe}^+ - u_b^+), \tag{5}$$

$$\tau^- = \frac{G}{t_s}(u_b^- - u_{pe}^-), \tag{6}$$

where E_b – Young's modulus of beam , E_{pe} – Young's modulus of the piezo-actuator, G – Kirchhoff's modulus of bonding layer. The geometric relation on the beam surface leads to

$$w_{,xx} = -\frac{2}{t_b}u_{b,x} = -\frac{2}{t_b}\varepsilon_b. \tag{7}$$

The bending moment M generated by the distributed normal stresses over the bem cross-section is equal to

$$M = \frac{t_b^2 b}{6}\sigma_b = \frac{E_b t_b^2 b}{6}\varepsilon_b. \tag{8}$$

Eliminating displacements w, u_{pe}^+, u_{pe}^-, inner forces and shear stresses τ^+, τ^- we can write beam surface and piezoelectric strains dynamic equations (2) and (4) for section 2 in the following form

$$\rho_{pe}t_{pe}\varepsilon_{,tt}^+ - E_{pe}t_{pe}\varepsilon_{,xx}^+ + \frac{G}{t_s}\left(\varepsilon^+ - \varepsilon_b\right) = 0, \qquad x \in (x_1, x_2), \tag{9}$$

$$\rho_{pe}t_{pe}\varepsilon_{,tt}^- - E_{pe}t_{pe}\varepsilon_{,xx}^- + \frac{G}{t_s}\left(\varepsilon_b - \varepsilon^-\right) = 0, \qquad x \in (x_1, x_2), \tag{10}$$

$$\rho_b^* \varepsilon_{b,tt} + \frac{E_b t_b^2}{12}\varepsilon_{b,xxxx} + \frac{G t_b}{4 t_s}\left(\varepsilon_{,xx}^+ - \varepsilon_{,xx}^- - 2\varepsilon_{b,xx}\right) = 0, \qquad x \in (x_1, x_2). \tag{11}$$

In the third section $x_2 < x < x_3$ the moment equation has modified form due to the lack of shear between the beam and the lower actuator and we obtain the two coupled partial differential equations of the form

$$\rho_{pe}t_{pe}\varepsilon_{,tt}^+ - E_{pe}t_{pe}\varepsilon_{,xx}^+ + \frac{G}{t_s}\left(\varepsilon^+ - \varepsilon_b\right) = 0, \qquad x \in (x_2, x_3), \tag{12}$$

$$\rho_b^* \varepsilon_{b,tt} + \frac{E_b t_b^2}{12}\varepsilon_{b,xxxx} + \frac{G t_b}{4 t_s}\left(\varepsilon_{,xx}^+ - \varepsilon_{b,xx}\right) = 0, \qquad x \in (x_2, x_3). \tag{13}$$

The motion of the beam in the first and fourth section is described by the classical Bernoulli–Euler equation, which can be obtained by neglecting the third term in Eq. (13)

$$\rho_b \varepsilon_{b,tt} + \frac{t_b^2}{12}\varepsilon_{b,xxxx} = 0, \qquad x \in (0, x_1) \cup (x_3, \ell). \tag{14}$$

The stress-strain relationship for the piezoelectric material has the form

$$\sigma_{pe} = E_{pe}\left(u_{pe,x} - \Lambda\right), \tag{15}$$

where the piezoelectric strain, the piezoelectric constant, and the applied voltage are denoted by $\Lambda = d_{31}\mathcal{V}/t_{pe}$, d_{31} and $\mathcal{V}$, respectively.

2.2. Boundary and joint conditions

We assume simply supported boundary conditions imposed on the solution of Eq. (14) at $x = 0$ and $x = \ell$, continuity of deflection, slope, curvature and transverse force for $x = x_1$, $x = x_2$ and $x = x_3$ as well as continuity of upper actuator displacement and upper actuator stress for $x = x_2$. The continuity condition of transverse forces should take into account the presence of the shear stresses τ^+, τ^-, e.g. for $x = x_1$ we have

$$E_b \frac{bt_b^3}{12} w_{,xxx}(x_1^-) = E_b \frac{bt_b^3}{12} w_{,xxx}(x_1^+) - \frac{t_b b}{2} \left(\tau^+(x_1^+) - \tau^-(x_1^+) \right), \tag{16}$$

and for $x = x_2$

$$E_b \frac{bt_b^3}{12} w_{,xxx}(x_2^-) - \frac{t_b b}{2} \left(\tau^+(x_2^-) - \tau^-(x_2^-) \right) = E_b \frac{bt_b^3}{12} w_{,xxx}(x_2^+) - \frac{t_b b}{2} \tau^+(x_2^+). \tag{17}$$

Solutions should satisfy free edge conditions corresponding to the zero normal stresses at the ends of piezo-actuators, which can be written in the form

$$\sigma_{pe}^+(x_1^+) = \sigma_{pe}^-(x_1^+) = \sigma_{pe}^+(x_3^-) = \sigma_{pe}^-(x_2^-) = 0. \tag{18}$$

Finally, full system of boundary and joint conditions have the form

$$w(0,t) = w(\ell,t) = 0, \qquad w_{,xx}(0,t) = w_{,xx}(\ell,t) = 0, \tag{19}$$

$$w(x_1^-,t) = w(x_1^+,t), \qquad w(x_2^-,t) = w(x_2^+,t), \qquad w(x_3^-,t) = w(x_3^+,t), \tag{20}$$

$$w_{,x}(x_1^-,t) = w_{,x}(x_1^+,t), \qquad w_{,x}(x_2^-,t) = w_{,x}(x_2^+,t), \qquad w_{,x}(x_3^-,t) = w_{,x}(x_3^+,t), \tag{21}$$

$$w_{,xx}(x_1^-,t) = w_{,xx}(x_1^+,t), \qquad w_{,xx}(x_2^-,t) = w_{,xx}(x_2^+,t),$$
$$w_{,xx}(x_3^-,t) = w_{,xx}(x_3^+,t), \tag{22}$$

$$T(x_1^-,t) = T(x_1^+,t), \qquad T(x_2^-,t) = T(x_2^+,t), \qquad T(x_3^-,t) = T(x_3^+,t), \tag{23}$$

$$\varepsilon^+(x_1^+,t) = \varepsilon^+(x_3^-,t) = \Lambda, \qquad \varepsilon^-(x_1^+,t) = \varepsilon^-(x_2^-) = -\Lambda, \tag{24}$$

$$u_{pe}^+(x_2^-,t) = u_{pe}^+(x_2^+,t), \qquad \varepsilon^+(x_2^+,t) = \varepsilon^+(x_2^-,t). \tag{25}$$

2.3. Steady-state solution

Assuming a harmonic single frequency excitation $\Lambda = \Lambda_0 \exp(i\omega t)$, steady-state responses of dynamic equations (9)-(15) are sought as harmonics with the same angular velocity

$$\begin{bmatrix} \varepsilon^+(x,t) \\ \varepsilon^-(x,t) \\ \varepsilon_b(x,t) \end{bmatrix} = \begin{bmatrix} \varepsilon^+(x) \\ \varepsilon^-(x) \\ \varepsilon_b(x) \end{bmatrix} \exp(i\omega t). \tag{26}$$

Substituting Eq. (26) into Eqs. (9)-(15), we obtain the system of ordinary differential equations solutions of which have the form dependent on the section number.

Section 1

$$\varepsilon_b(x) = C_1 \exp(k_1 x) + C_2 \exp(-k_1 x) + C_3 \exp(ik_1 x) + C_4 \exp(-ik_1 x), \qquad (27)$$

where

$$k_1 = \sqrt[4]{\frac{12\rho_b\omega^2}{E_b t_b^2}}.$$

Section 2

$$\varepsilon_b(x) = \sum_{n=7}^{12} C_n \alpha(k_n, \omega) \exp(k_n x), \qquad (28)$$

$$\varepsilon^+(x) = C_5 \exp(k_5 x) + C_6 \exp(-k_5 x) + \sum_{n=7}^{12} C_n \exp(k_n x),$$

$$\varepsilon^-(x) = C_5 \exp(k_5 x) + C_6 \exp(-k_5 x) - \sum_{n=7}^{12} C_n \exp(k_n x), \qquad (29)$$

where

$$k_5 = \sqrt{\frac{G}{t_s t_{pe} E_{pe}} - \frac{\rho_{pe}}{E_{pe}}\omega^2},$$

the wavenumbers k_i, $i = 7, \ldots, 12$, satisfy the following algebraic equation

$$k^6 \frac{E_b t_b^2}{12} E_{pe} t_{pe} + k^4 \left[\rho_{pe} \frac{E_b t_b^2 t_{pe}}{12} \omega^2 - \frac{G t_b}{2 t_s} \left(\frac{E_b t_b}{6} + E_{pe} t_{pe} \right) \right]$$
$$- k^2 \omega^2 \left(\rho_{pe} \frac{t_{pe} t_b G}{2 t_s} + \rho_b^* E_{pe} t_{pe} \right) - \rho_b^* \omega^2 \left(\rho_{pe} t_{pe} \omega^2 - \frac{G}{t_s} \right) = 0 \quad (30)$$

and

$$\alpha(k, \omega) = 1 - \frac{E_{pe} t_c t_s}{G} k^2 - \frac{\rho_{pe} t_c t_s}{G} \omega^2.$$

Section 3

$$\varepsilon_b(x) = \sum_{n=13}^{18} C_n \alpha(k_n, \omega) \exp(k_n x), \varepsilon^+(x) = \sum_{n=13}^{18} C_n \exp(k_n x), \qquad (31)$$

where the wavenumbers k_i, $i = 13, \ldots, 18$, satisfy the following algebraic equation

$$k^6 \frac{E_b t_b^2}{12} E_{pe} t_{pe} + k^4 \left[\rho_{pe} \frac{E_b t_b^2 t_{pe}}{12} \omega^2 - \frac{G t_b}{4 t_s} \left(\frac{E_b t_b}{3} + E_{pe} t_{pe} \right) \right]$$
$$- k^2 \omega^2 \left(\rho_{pe} \frac{t_{pe} t_b G}{4 t_s} + \rho_b^* E_{pe} t_{pe} \right) - \rho_b^* \omega^2 \left(\rho_{pe} t_{pe} \omega^2 - \frac{G}{t_s} \right) = 0. \quad (32)$$

Section 4

$$\varepsilon_b(x) = C_{19} \exp(k_1 x) + C_{20} \exp(-k_1 x) + C_{21} \exp(ik_1 x) + C_{22} \exp(-ik_1 x). \qquad (33)$$

The twenty two unknown coefficients $C_1, C_2, \ldots, C_{22}$ are determined by the boundary and joint conditions described by Eqs. (19)-(25).

2.4. Results

Numerical calculations based on the formulae presented in the previous sections are performed for $\omega = 0.1$ 1/s for the static loading, and in the first beam resonance region $\omega = 206$ 1/s, and and $\Lambda = 0.001$. The dimensions of the steel beam are $\ell = 380$ mm, width $b = 40$ mm and thickness $t_b = 2$ mm. The piezoelectric actuators are located between $x_1 = 0.079\,m$ and $x_3 = 0.117\,m$. The remaining dimensions are width $b = 40$ mm and thickness $t_{pe} = 0.2$ mm. The center of the piezoelectrics is located at $x = 98$ mm. The parameters of the beam and piezoelectric elements used in calculations are listed in Table 1. The mass per unit area ratio of the piezoelement and the beam is equal to 0.55. As there is no precise data available relating the Kirchhoff modulus G of bonding layer, and the bonding layer thickness t_s calculations are performed for the following values of parameter $G/t_s = 10^{10}, 10^{11}$ corresponding to the soft and the intermediate bonding, respectively. The main parameter is the relative length of delamination, where 0 corresponds to the no delamination. The dynamic characteristics are calculated for the four values of relative length of delamination of the lower actuator 0, 0.25, 0.5, and 0.75.

TABLE 1. Material parameters used in calculations.

Material	Beam–Steel	Actuator–PZTG-1195
ρ, kg/m^3	7800	7275
E, N/m^2	21.6×10^{10}	63×10^9
t m	0.002	0.0006
d_{31}, m/V	–	1.9×10^{-10}

Figure 3 shows the beam responses to a cyclic piezoelectric strains applied to the piezoelectric actuators bonded to the beam in $x = 0.1$ m. The magnitude of the transfer functions decreases as the delamination length increases.

It is seen that the presence of delamination does not significantly decrease the first natural frequency. Figures 4 and 5 show that the effect of delamination length does not change qualitatively the spatial distribution of beam displacement in the first resonance region as the bonding layer parameter G/t_s increases. It is observed that the delamina-
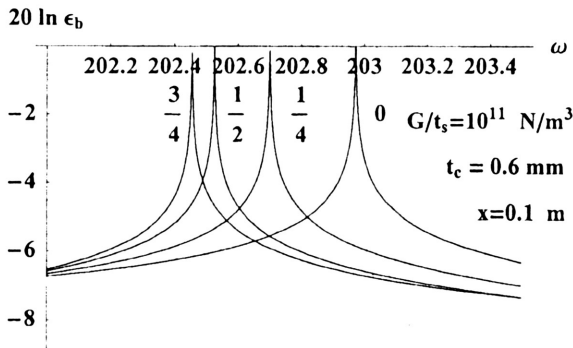

FIGURE 3. Near field beam transverse response ε_p at $x = 0.1$ m in the first beam resonance.

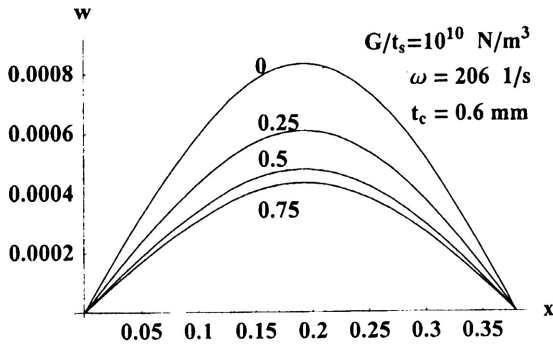FIGURE 4. Influence of relative delamination length on spatial beam displacement for soft bonding
layer $G/t_s = 10^{10}$ N/m^3.
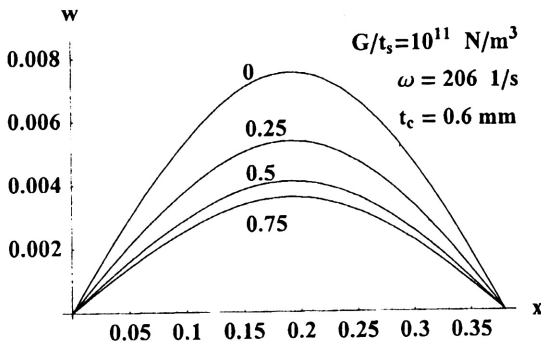

FIGURE 5. Influence of relative delamination length on spatial beam displacement for intermediate
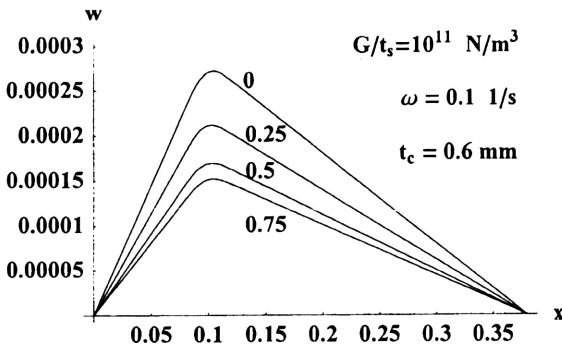bonding layer $G/t_s = 10^{11}$ N/m^3.

FIGURE 6. Influence of relative delamination length on spatial beam displacement for quasistatic
excitation $\omega = 0.1$ 1/s.

tion decreases piezo-actuator coupling performance independently of the bonding layer stiffness. It is seen that if the bonding layer parameter is increased the beam deflection increases. But the increase is more pronounced at small values of G/t_s.

Comparison of Figs. 5 and 6 show different spatial responses for different excitation frequencies. Figure 6 shows the beam deflection at $\omega = 0.1$ 1/s corresponding to a very slow excitation (static loading). As the inertia forces are negligible and there are no external forces in the first and the forth section the curvature is equal to zero and displacements are represented by straight lines. Due to the shear stresses in the second and the third section we have a curve with the nonzero curvature. Integrating strains $\varepsilon^+, \varepsilon^-, \varepsilon_b$ with respect to x and using Eqs. (5)-(6) yield the shear stresses in the bonding layers.

Section 2 $(x_1 < x < x_2)$

$$\tau^+ = \frac{G}{t_s}\left(\frac{C_5 \exp(k_5 x) - C_6 \exp(-k_5 x)}{k_5} + \sum_{n=7}^{12} \frac{C_n}{k_n}\left(1 - \alpha(k_n,\omega)\right)\exp(k_n x)\right), \quad (34)$$

$$\tau^- = \frac{G}{t_s}\left(\frac{-C_5 \exp(k_5 x) + C_6 \exp(-k_5 x)}{k_5} + \sum_{n=7}^{12} \frac{C_n}{k_n}\left(1 - \alpha(k_n,\omega)\right)\exp(k_n x)\right). \quad (35)$$

Section 3 $(x_2 < x < x_3)$

$$\tau^+ = \frac{G}{t_s}\sum_{n=13}^{18} \frac{C_n}{k_n}\left(1 - \alpha(k_n,\omega)\right)\exp(k_n x), \qquad \tau^- = 0. \quad (36)$$

Figures 7, 8 show the distributions of shear stress along the second and third sections as functions of x and the bonding layer parameter. The shear stress calculated according to present theory (Eqs. (34)-(36)) can be compared with the static shear stress for bonded piezo-actuators without delamination [3] denoted by a dashed curve.

The present dynamic analysis and the static one are in a qualitative agreement. The shear stresses are antisymmetric with respect to the center of piezoelectric actuator. But the absolute values of the dynamic shear stresses are larger. For large G/t_s the stress
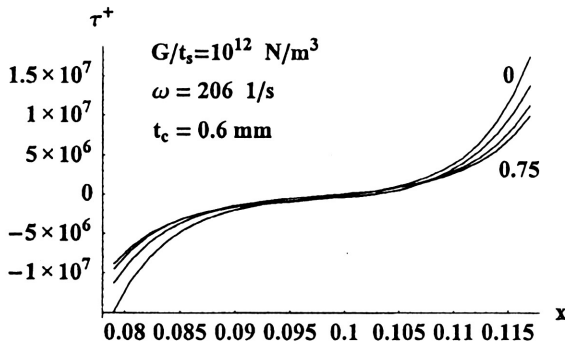

FIGURE 7. Shear stress distribution in the upper bonding layer (no delamination) at $\omega = 206$ 1/s.
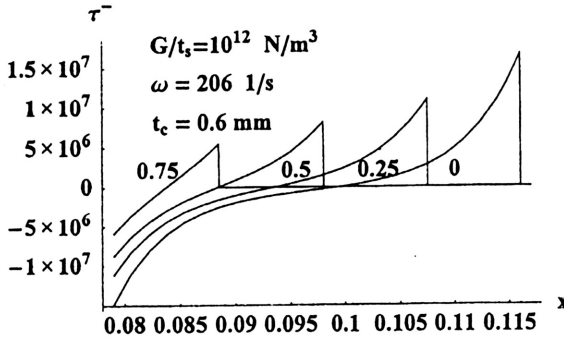
FIGURE 8. Shear stress distribution in the lower bonding layer (delamination) at $\omega = 206$ 1/s.
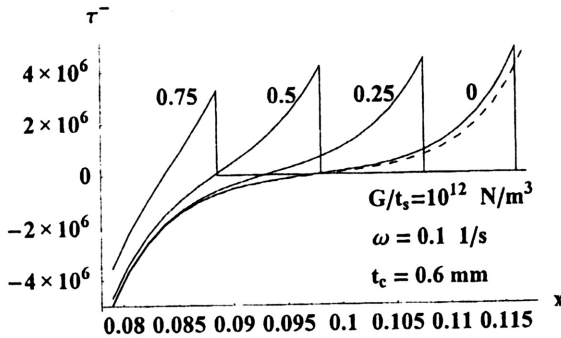

FIGURE 9. Comparison of shear stress distributions in the upper bonding layer for low frequency excitation $\omega = 0.1$ 1/s.

distribution gathers in the regions close to the piezo-actuator ends and converges to the distribution described by a linear form of the δ-Dirac functions concentrated at the piezoelement ends [1]. Comparison of the shear stresses for slowly varying excitations $\omega = 0.1$ 1/s calculated according the present dynamical approach (continuous line) and the static model [3] (dashed line) shows a good agreement (Fig. 9). The spatial dynamic stress distributions in the upper bonding layer and in the lower bonding layer are shown in Figs. 7, 8, respectively.

It is seen that the delamination qualitatively changes the stress distribution in the delamination region decreasing the performance of the lower piezo-actuator. Despite the zero shear stresses in the third section of lower layer the increase of the shear stresses in the upper perfectly bonding layer is not observed.

2.5. Conclusions

A dynamic model has been developed which is able to predict the response of a beam driven by the piezoelectric actuators glued to lower and upper beam surfaces. The actuators are driven by a pair of electrical fields with the same amplitude and in

opposite phase. The actuators were used to excite steady-state harmonic vibrations in the beam. The results obtained from this analysis are compared with particular cases from past studies, which were based on the assumption of static coupling between the actuator and the beam. The numerical tests performed for the simply supported beam with surface bonded actuators show the influence of the delamination on the vibration characteristics. The increase of edge delamination decreases the magnitude of transfer functions between the applied voltage to the piezo-actuators and the displacement of a fixed point of beam, and the shear stresses in the bonding layer, and the surface beam strains. The presented analytical model is a handy tool to the fast introductory obtaining of different dynamical characteristics of controlled structures with piezo-actuators. The results can be applied to at least qualitative evaluation of the delamination harmful effect on piezo-actuator coupling performance.

3. Flexural vibrations of shafts with delaminations

Effects on the eigenfrequencies due to delamination in a composite rotor were studied in [13]. The influence of position and varying size of imperfection on the eigenfrequencies is examined using finite element model of cylindrical shaft. Consider a general model of laminated rotating shaft with circumferential delaminations [12]. The shaft is treated as a thin-walled composite cylindrical shell. The delamination of constant width is parallel to the shell reference surface and it covers the entire circumference. The edge delamination is modeled by changing the effective reduced stiffnesses of debonded parts. The stabilizing effect of external damping and destabilizing effect of internal damping are taken into account in the dynamic stability analysis.

3.1. Problem formulation

The shaft is treated as a thin laminated shell of the length ℓ, the mean radius R and the total thickness h consisting of an even number of equal thickness orthotropic layers symmetrically cross-ply arranged about its midsurface. The Kirchhoff hypothesis on nondeformable normal element is assumed. Rotary and coupling inertias are neglected. The motion of the shell is compound of a rotary motion with a constant angular velocity Ω and the relative motion described by vector components u, v, w in tangential, circumferential, and radial direction, respectively. The rotating coordinate system is connected with an undeformed midsurface of the shell. The shell is assumed to be simply supported with axially movable ends at $x = 0$ and $x = \ell$. We have also continuity conditions at $y = 0$ and $y = 2\pi R$ as the considered shell is a closed shell. It is assumed that in the vibrating shaft the delamination of the length d does not expand and bending stiffnesses are described by step function of the longitudinal coordinate x. The position in the radial direction is given by s measured from the external shell surface. The dynamic equations of shell motion are given in the following form

$$u_{,tt} + 2\beta u_{,t} - a_{11}u_{,xx} - a_{66}u_{,yy} - (a_{12} + a_{66})v_{,xy} - \frac{a_{12}}{R}w_{,x} = 0, \qquad (37)$$

$$v_{,tt} + 2\Omega w_{,t} - \Omega^2 v + 2\beta v_{,t} + 2\beta_e \Omega w - (a_{12} + a_{66})u_{,xy} - a_{66}v_{,xx} - a_{22}v_{,xx} - \frac{a_{22}}{R}w_{,y} = 0, \quad (38)$$

$$w_{,tt} - 2\Omega v_{,t} - \Omega^2 w + 2\beta w_{,t} + 2\beta_e \Omega v + \frac{a_{12}}{R} u_{,x} + \frac{a_{22}}{R} v_{,y} + d_{11} w_{,xxxx}$$

$$+ 2(d_{12} + 2d_{66}) w_{,xxyy} + d_{22} w_{,yyyy} + \frac{a_{22}}{R^2} w - R^2 \Omega^2 w_{,yy} = 0, \qquad (x,y) \in \mathcal{D}, \quad (39)$$

where reduced stiffnesses $a_{11}, \ldots, d_{66}$ are the laminate stiffnesses $A_{11}, \ldots, D_{66}$ divided by ρh, β_i, and β_e are reduced damping coefficients in relative and absolute motion, respectively, and ρ is the mean density of the shell material, $\beta = \beta_i + \beta_e$.

3.2. Stability analysis

The purpose of the present paper is to examine the influence of edge delamination on the stability region expressed by an critical angular velocity. In order to examine the Liapunov stability of trivial solution $u = v = w = 0$ an energy-like functional is introduced [10] in the form

$$\mathcal{V} = \frac{1}{2} \int_{\mathcal{D}} \left\{ (u_{,t} + 2\beta u)^2 + (v_{,t} + 2\beta v)^2 + (w_{,t} + 2\beta w)^2 + u_{,t}^2 + v_{,t}^2 + w_{,t}^2 \right.$$

$$- 2\Omega^2 (v^2 + w^2) + 2 \left[a_{11} u_{,x}^2 + a_{22} \left(v_{,y} + \frac{w}{R} \right)^2 + 2a_{12} u_{,x} \left(v_{,y} + \frac{w}{R} \right) + a_{66} (u_{,y} + v_{,x})^2 \right.$$

$$\left. \left. + d_{11} w_{,xx}^2 + 2d_{12} w_{,xx} w_{,yy} + d_{22} w_{,yy}^2 + 4d_{66} w_{,xy}^2 \right] + 2R^2 \Omega^2 w_{,y}^2 \right\} d\mathcal{D}. \quad (40)$$

The time-derivative of Liapunov functional along solutions of the dynamics equation is given by

$$\frac{d\mathcal{V}}{dt} = -2\beta \int_{\mathcal{D}} \left\{ u_{,t}^2 + \left(v_{,t} - \Omega\sqrt{\varepsilon} w \right)^2 + \left(w_{,t} + \Omega\sqrt{\varepsilon} v \right)^2 - \Omega^2 (1 + \varepsilon)(v^2 + w^2) \right.$$

$$+ a_{11} u_{,x}^2 + a_{22} \left(v_{,y} + \frac{w}{R} \right)^2 + 2a_{12} u_{,x} \left(v_{,y} + \frac{w}{R} \right) + a_{66} (u_{,y} + v_{,x})^2$$

$$\left. + d_{11} w_{,xx}^2 + 2d_{12} w_{,xx} w_{,yy} + d_{22} w_{,yy}^2 + 4d_{66} w_{,xy}^2 + R^2 \Omega^2 w_{,y}^2 \right\} d\mathcal{D} \le 0, \quad (41)$$

where $\varepsilon = (\beta_i/\beta)^2$. The functional $\mathcal{V}$ is positive definite if the angular velocity is sufficiently small. Then, the measure of distance between arbitrary solutions of Eqs. (37)-(39) and the trivial one can be chosen as the square root of the Liapunov functional. Using results of numerical calculations of the free vibration frequencies it is easy to find a constant δ satisfying the following variational inequality

$$\int_{\mathcal{D}} \left[d_{11} w_{,xx}^2 + 2d_{12} w_{,xx} w_{,yy} + d_{22} w_{,yy}^2 + 4d_{66} w_{,xy}^2 \right] d\mathcal{D} \ge \delta \int_{\mathcal{D}} w^2 d\mathcal{D}. \qquad (42)$$

Critical parameters can be found by examining the positive-definiteness of the functional time-derivative. As the shell is used to model the rotating transmission shaft with the large aspect ratio ($\ell/R \gg 1$) bending modes of vibration dominate. Using the standard stability analysis we obtain stability conditions. Substituting Eq. (42) into the stability

condition (41) we see that the non-positive definiteness of the functional time-derivative is equivalent to positiveness of the following matrix

$$\begin{bmatrix} a_{11} & a_{12} & a_{12} \\ a_{12} & a_{22} - R^2\Omega^2(1+\varepsilon) & a_{22} \\ a_{12} & a_{22} & a_{22} + \delta R^2 - R^2\Omega^2\varepsilon \end{bmatrix}. \tag{43}$$

3.3. Results

The critical angular velocity of rotating shaft with seven graphite-epoxy cross-ply layers are calculated using Sylvester conditions to the matrix (43). The critical parameter $R^2\Omega^2$ depends on the relative delamination length d/ℓ and the relative radial position s/h. The dimensions of the graphite-epoxy shell are $\ell = 1\,\text{m}$, $R = 0.03\,\text{m}$, $h = 0.005\,\text{m}$. For an orthotropic lamina engineering constants are $E_L = 2.11 \cdot 10^{11}\,\text{Pa}$, $E_T = 0.053 \cdot 10^{11}\,\text{Pa}$, $G_{LT} = 0.026 \cdot 10^{11}\,\text{Pa}$, $\nu_{LT} = 0.25$, $\rho = 1560\,\text{kg/m}^3$. The damping ratio ε is equal to 0.5 It is seen that the delamination length is mainly responsible for the decrease of the critical parameter.

TABLE 2. Critical stability parameter $R^2\Omega^2$ vs. the relative delamination length and the radial position of the delamination.

d/ℓ s/h	0.0	0.1	0.2	0.3	0.4	0.5	0.6	0.7
2/7	1336.3	1314.5	1156.7	887.2	635.0	487.6	431.8	417.9
3/7	1336.3	1315.6	1161.1	898.4	652.5	508.7	454.4	440.8

Acknowledgements

References

1. T. Bailey and J.E. Hubbard, *Distributed piezoelectric-polymer active vibration control of a cantilever beam*, Journal of Guidance, Control and Dynamics, Vol.8, pp.605-611, 1985.

2. A. Bogdanovich and N. Rastogi, *3-D variational analysis of bonded composite plates*, Proceedings of the ASME Aerospace Division, Vol.52, ASME, pp.123-143, 1996.

3. E.F. Crawley and J. de Luis, *Use of piezoelectric actuators as elements of intelligent structures*, AIAA J., Vol.25, pp.1373-1385, 1987.

4. W. Jiang and G. Bao, *Delamination induced buckling in orthotropic plate structures*, Proceedings of the ASME Aerospace Division, Vol.52, ASME, pp.31-38, 1996.

5. Jie Pan, C.H. Hansen and S.D. Snyder, *A study of the response of a simply supported beam to excitation by piezoelectric actuator*, [in:] C.A. Rogers and C.R. Fuller [eds.], Recent Advances in Active Control of Sound and Vibration, Technomic Publishing, Lancaster-Basel, pp.39-49, 1991.

6. P.M. Mujumdar and S. Suryanarayan, *Flexural vibrations of beams with delaminations*, Journal of Sound and Vibrations, Vol.125, pp.441-461, 1988.

7. M.J. Newman, *Distributed active vibration controllers*, [in:] C.A. Rogers and C.R. Fuller [eds.], Recent Advances in Active Control of Sound and Vibration, Technomic Publishing, Lancaster-Basel, pp.579-592, 1991.

8. Sung Jin Kim and J.D. Jones, *Effects of piezo-actuator delamination on the performance of active noise and vibration control systems*, DSC, Vol.38, Active Control of Noise and Vibration, ASME, pp.213-221, 1992.

9. A. Tylikowski, *Stabilization of beam parametric vibrations*, Journal of Theoretical and Applied Mechanics, Vol.31, pp.657-670, 1993.

10. A. Tylikowski, *Dynamic stability of rotating composite shells with thermoactive shape memory alloy fibers*, J. Thermal Stresses, Vol.21, pp.327–339, 1998.

11. A. Tylikowski, *Effects of piezo-actuator delamination on the transfer functions of vibration control systems*, Int. J. of Solids and Structures, Vol.38, 2189-2202, 2001.

12. A. Tylikowski, *Flexural vibrations of rotating shafts with delaminations*, GAMM Meeting – Book of Abstracts, Zürich, p. 151, 2001.

13. H.L. Wettergren, *Delamination in composite rotors*, Composites Part A, Vol.28A, pp.523-527, 1997.

————◇————